

Influence of the axial force on the behavior of endplate moment connections

Mehdi Ghassemieh^{1a}, Iman Shamim^{2b} and Ali Akbar Gholampour^{*1}

¹*School of Civil Engineering, University of Tehran, Tehran, Iran*

²*Department of Civil Engineering and Applied Mechanics, McGill University, Canada*

(Received March 5, 2012, Revised October 18, 2013, Accepted December 9, 2013)

Abstract. In this article, using finite element method of analysis (FEM), behavior of the endplate moment connection subjected to axial force and bending moment is investigated. In the FEM model, all the nonlinear characteristics such as material, geometry, as well as contact have been included. First, in order to verify the numerical model of the connection, an analysis of the endplate moment connection conducted without the application of the axial force. Results obtained from FEM indicating a close and good correlation with the experimental results. Then to investigate the influence of the axial forces, the connections subjected to axial forces as well as the bending moment are analyzed. To observe the overall effect of these actions, the moment-axial force interaction diagrams are drawn. It is observed that the presence of axial force even in a small value can change the behavior of the connection significantly. It is also shown that the axial forces can alter the failure mode of the connection; and therefore it could result in a different than the predicted moment capacity of the connection.

Keywords: moment connection; endplate; axial loading; finite element method; extended connection

1. Introduction

The endplate moment connection consists of a plate welded to the end of the connecting beam and then bolted to the connecting column using rows of high strength bolts. These types of connections are basically used to connect beam to column and sometimes to splice two beams together as shown in Fig. 1.

There are two main types of endplate moment connections; being flush or extended. The flush endplate moment connection consists of an endplate that is cut outside of the connecting beam flanges and all bolts are positioned between the flanges. Extended endplate moment connection contains an endplate extended outside of the beam flanges; and at least one bolt row is positioned in the extended region of the plate. Extended endplate can be stiffened or unstiffened (Fig. 2). Stiffened configuration has stiffeners welded to outside part of the beam flange and stiffener is aligned with the web of the beam to strengthen the extended part of the endplate.

In the frames subjected to wind or earthquake, the axial forces develop in the connection due to

*Corresponding author, Ph.D. Candidate, E-mail: aagholampour@ut.ac.ir

^aAssociate Professor, E-mail: mghassem@ut.ac.ir

^bPh.D. Candidate, E-mail: iman.shamim@mail.mcgill.ca

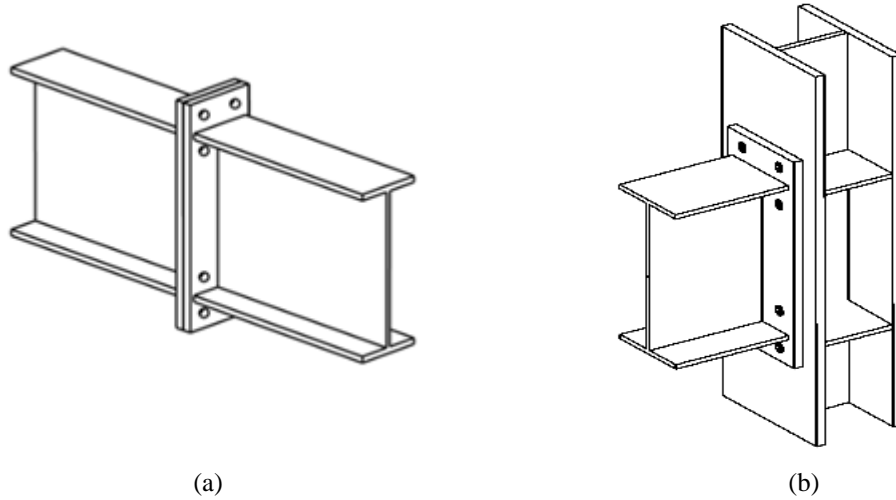


Fig. 1 Typical endplate moment connections (a) Beam splice connection, (b) Beam to column connection

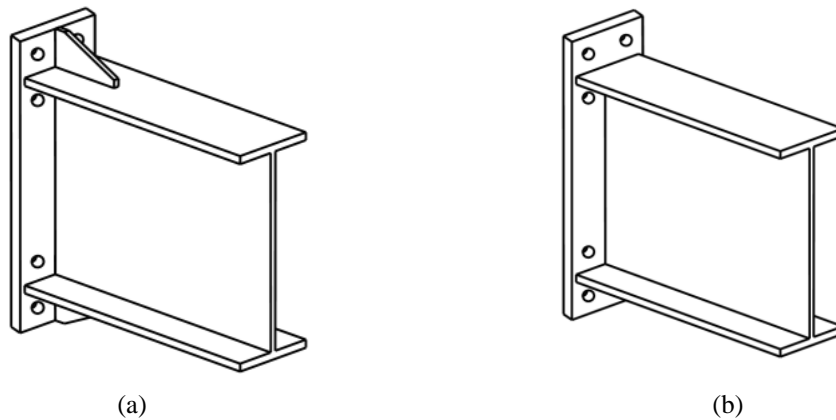


Fig. 2 Extended endplate connections (a) Stiffened, (b) Unstiffened

lateral loads. The axial forces as well as the bending moments may also take place simultaneously in the beam to column joints, beam splices and/or in pitched roof frame joints. These axial forces may be of tensile or compressive type and as the lateral load direction changes, normally the type of axial forces changes as well. The application of the axial force in the endplate moment connection along with the existence of the bending moment due to gravity loads as well as lateral loads can result in altering the behavior of the entire connection.

Many investigators studied the behavior of the endplate connections under different circumstances; but few looked into the effect of axial forces on such connections. Sherbourne (1961) conducted five tests on the connection with endplate and concluded that the rotational capacity of connection which has been produced from plastic deflection of endplate is sufficient. Mann (1968) applied six tests on endplate connection and proposed equations for prediction of endplate strength. Krishnamurthy and Graddy (1976) conducted one of the earliest studies on the endplate moment

connection using finite element analysis. In their studies, thirteen connections were analyzed by 2D-3D program. Ahuja *et al.* (1982) investigated the elastic behavior of the eight-bolt extended endplate connection using FEM. Ghassemieh *et al.* (1983) investigated the nonlinear behavior of the endplate moment connection for the first time. For that reason, eight prototype connections were tested and also the 2D-3D FEM program was developed and the analytical and experimental results were obtained and compared with each other. Bahari and Sherbourne (1994) used ANSYS computer program to analyze 3D models that predicted the behavior of the endplate moment connection successfully. Bose *et al.* (1997) applied the FEM to analyze two bolted and four bolted flush endplate moment connections. In their study, a good correlation attained in comparison with their experimental results. Meng (1996) used shell element for modeling the behavior of bending connection with unstiffened four bolted extended endplate. The FEM results had good correlation with the experiment results. Bond and Murray (1989) conducted tests on the flush endplates in order to come up with design methodology of such connections. Mays (2000) used FEM analysis for design of stiffened 16 bolted extended endplate and flange of unstiffened column. Murray (1990, 2002) managed to propose the design equations for the extended endplate moment connections, which was ultimately included in the AISC specifications. Borgsmiller (1995) provided simple design equations for five different endplate type connections which included the effect of the pretensioning of the bolts on the prying force. Sumner and Murray (2001) studied the behavior of four-bolt extended unstiffened endplate moment connection subjected to cyclic loading. They also studied the influence of changes in the web height of column and endplate thickness on the connection behavior. Adey *et al.* (1998, 2000) conducted tests on extended endplate moment connections subjected to cyclic loading. Their test results indicated that an increase in endplate thickness results in increased average energy absorption per inelastic excursion but may not result in an increase in total energy absorption. Also they proposed predicted equations which were applicable to stiffened and unstiffened endplate moment connections with various bolt layouts. Nogueiro *et al.* (2009) worked on calibration of model parameters for the cyclic response of endplate beam-to-column steel-concrete composite joints. Aggarwal (1994) conducted tests carried out on beam to column joints with the aim of comparing the behavior of flush and extended endplate joints. It was observed that the flush endplate joints, though having rotations similar to the extended endplate joints, had lower load and moment carrying capacities. Coelho and Bijlaard (2007) investigated experimental behavior of high strength steel endplate connections. The test results had shown that the tested connections satisfy the design provisions for stiffness and resistance and achieve reasonable rotation demands. Yang and Kim (2007) investigated cyclic behavior of bolted and welded beam to column joints. Diaz *et al.* (2011) used FEM model of beam to column extended endplate joints. The results from the finite element analysis were verified by comparing the obtained moment-rotation curve of the joint. Coelho *et al.* (2004) studied experimental assessment of the ductility of extended endplate connections. The results shown that an increase in endplate thickness results in an increase in the connections flexural strength and stiffness and a decrease in rotational capacity. Lemonis and Gantes (2009) investigated mechanical modeling of the nonlinear response of beam to column joints. The proposed methodology was evaluated against experimental tests and finite element models in terms of stiffness, strength and rotational capacity, and its performance was found to be very satisfactory.

For the first time, Jaspert *et al.* (1999) considered the effect of normal forces along with bending moments on the skew type end plate moment connection. They developed a linear type interaction diagram between normal force and bending moment resistances for beam-to-column joints. Sokol *et al.* (2002) also developed similar interaction diagram through experimental as well as analytical

component method and finally they proposed the procedure to be adopted in EuroCode which was too conservative for non-symmetrical joints. Da Silva *et al.* (2004). De Lima *et al.* (2004), Da Silva (2008) investigated the behavior of the endplate beam to column joints subjected to bending and axial force experimentally as well as analytically using the component method. The results shown that the presence of an axial load on the beam significantly modifies the joint response. Urbonas and Daniunas (2006) investigated the behavior of semi-rigid steel beam-to-beam joints subjected to both bending as well as axial forces using the component method. They also indicated that the level of axial forces in joints of structures can be significant and have a significant influence on characteristics of semi-rigid joints.

Since few studies consider the impact of the axial forces on the behavior of the moment connections and only the minority on the end plate connections, therefore, the need to verify and study the interaction of the axial forces and the bending moments seems to be essential and required. Also the analytical methods used along with the experimental procedures mainly concentrated on the component methods that may hold some accuracy drawbacks. Thus, in this research, the effect of axial forces on the behavior of endplate moment connection is investigated using the finite element method of analysis. For this reason, in this study, ABAQUS (2003) was used as a main purpose computer program. All the nonlinear properties such as material, contact, large deformation, and buckling are included in the FEM model. Two different types of behavior are studied and analyzed. It is expected from some connections to have thick plate behavior, with the bolts becoming critical, and other connections to have intermediate or thin plate behavior, with the plate becoming critical. To put confidence in accuracy and precision of the FEM results, two connections that were tested by Maggi *et al.* (2004) were modeled first. Then the connections are subjected to monotonic load and the results obtained are compared with the existing experimental results. Then, for studying the axial force influence on the moment behavior of the connection, axial forces along with bending moment are applied on the connection. Both connections are designed weaker than the connecting beam intentionally in order to understand the behavior of the connection components at ultimate stage before occurrence of beam failure. Finally to display the effect of the axial forces on the behavior of such connections, the interaction diagram of axial forces and bending moments are obtained.

2. Finite element modeling

Two unstiffened endplate moment connections of extended type are modeled and analyzed. These connections were designed intentionally by Maggi *et al.* (2004) in such a way that it was expected from one to have the intermediate thickness endplate moment connection behavior (ct1b6 model), and from another to have thick endplate moment connection behavior (ct1a1 model). In the study done by Maggi *et al.* (2004), they have also conducted experiment on these connections subjected to bending moment only. As a first step in this study, the accuracy of the current FEM analysis can be verified by comparing the experimental results with the results obtained from FEM. The main purpose of this modeling are as follows; investigating the moment behavior of two types of connections, studying the accuracy of previously proposed theories, determining the strength and stiffness of the connections, and understanding how the tensile force is distributed along the bolt rows. The brick elements are used for meshing all parts of the connection model. Beam, endplates, column flange, and bolts are modeled with eight noded elements (C3D8I) which holds all the nonlinear properties. Beam, endplate, and column flange are all made with ASTM A36 steel, and

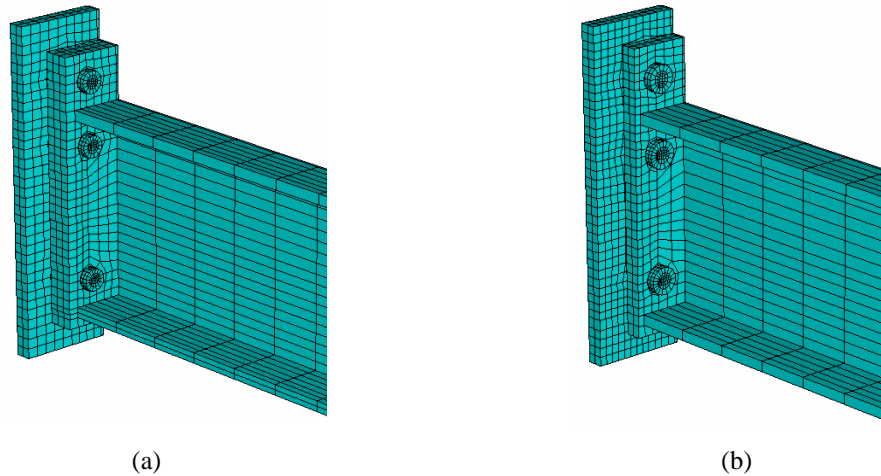


Fig. 3 Typical finite element mesh (a) ct1a1, (b) ct1b6

Table 1 Specifications and predicted resistant moments of ct1a1 and ct1b6 connections (Maggi *et al.* 2004)

	Endplate			Bolt	Resisting Moment (KN.m)	Resisting Moment (KN.m)	
	yield stress (MPa)	thickness (mm)	width (mm)			diameter (mm)	tensile strength (MPa)
ct1a1	288	31.5	155	16	712.56	136.04	501.49
ct1b6	288	19	145	19	712.56	191.93	160.9

bolts are A325 high strength bolts. Due to symmetry of loads and geometry, only half of the connection is modeled (Fig. 3).

This model is analyzed in proportion to the symmetric plane by using constraint conditions. The column web and its stiffeners are constrained; and therefore the column web is not modeled. In other words, the deformation of column web is ignored. Column flange width is considered to be 397 mm with 19 mm thickness. The beam, having 1.5 m length, welded to the endplate. Endplate and column flange surfaces are in contact. The bolt shank surfaces as well as endplate are also in contact. For creating bending moment, the uniform shear force is applied at the tip of the beam, and it is increased linearly until the solving process stops due to the connection failure. The failure of the connection is ascertained when one of the following criteria is taking place; a) the equivalent von Mises stress in the entire bolt (every node in the cross section) exceeds the maximum bolt stress rupture, b) initiation of the buckling in the compressive regions and c) excessive deformation in the endplate being around twelve yield strain of the steel material. The thermal loading is used for developing pretension forces in the bolts prior to any load application. The pretensioning stress in bolts is considered as 440 MPa which is about 70% of bolt yield strength. The configuration of two connections is shown in Fig. 4 and Table 1.

In Table 1, the moment capacity has been calculated from existing design equations from AISC (2005). In addition, the stress-strain relationship for the connection components is shown in Fig. 5. For bolts as well as endplate, trilinear stress-strain curve are implemented in the material model. It must be pointed that for the material model, isotropic hardening was employed, since the loading sequence was monotonic.

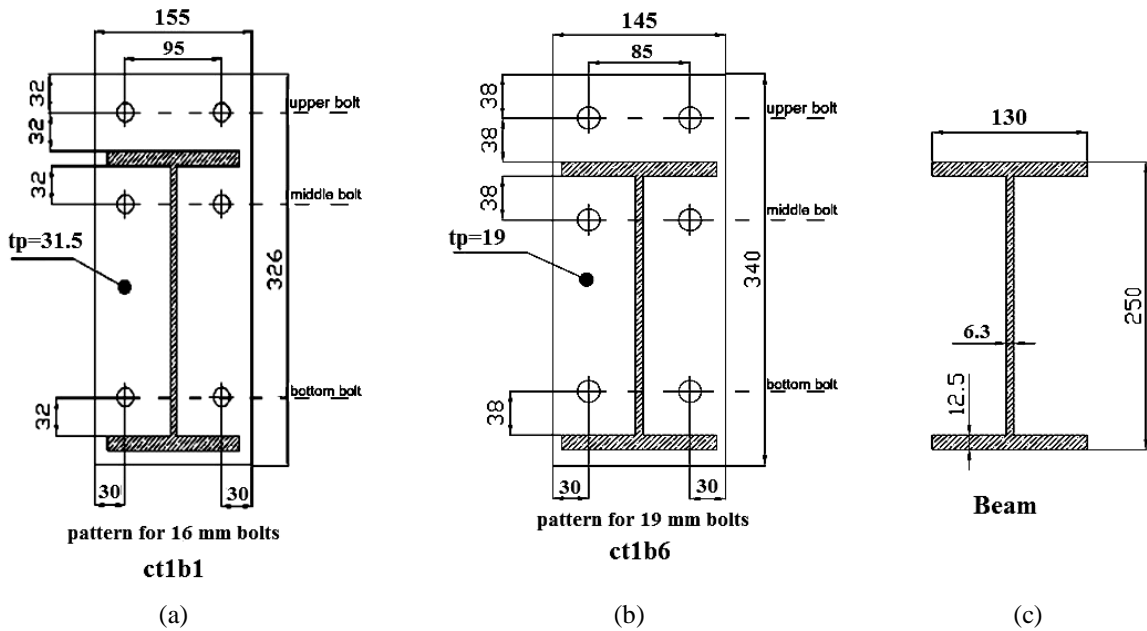


Fig. 4 Connections details (a) ct1a1, (b) ct1b6, and (c) beam (Maggi *et al.* 2004)

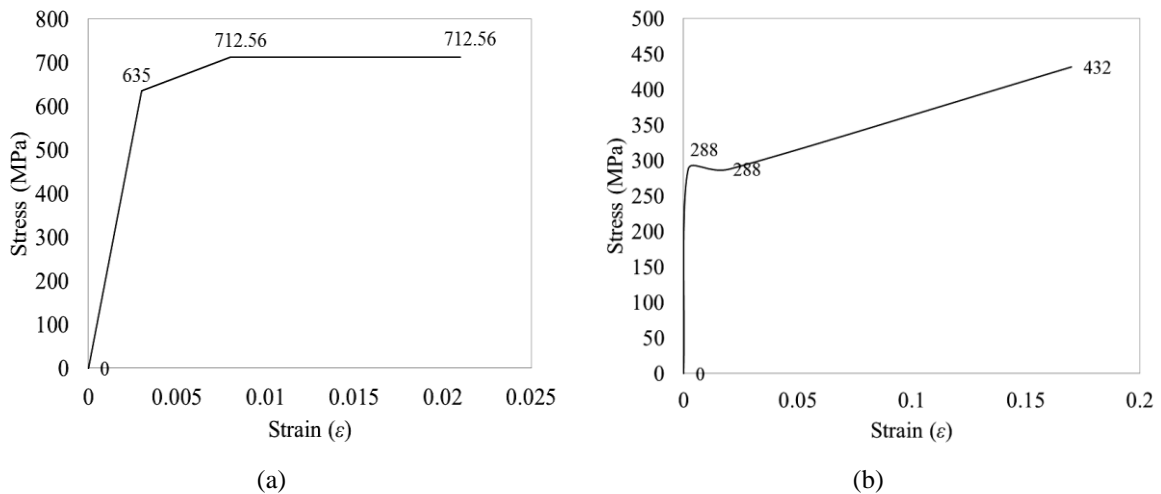


Fig. 5 Stress-strain relationship in (a) Bolts, (b) Beam, column, and endplate

3. Moment connection behavior without axial force

Before investigating the effect of axial loads on the overall behavior of the two aforementioned connections, and in order to verify the numerical model of the connection, an analysis of the endplate moment connection conducted without the application of the axial force.

Studying the bolt force during loading is a leading clue to investigate the moment connection behavior and understanding the connection failure mode. Thus, the tensile forces in the bolts need to

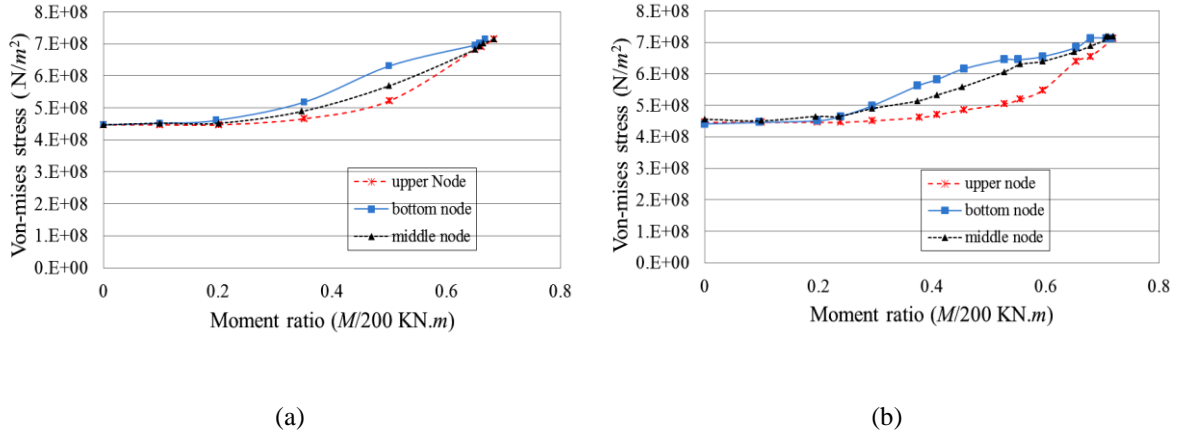


Fig. 6 Von-Mises stress vs. applied moment in (a) ct1a1, (b) ct1b6

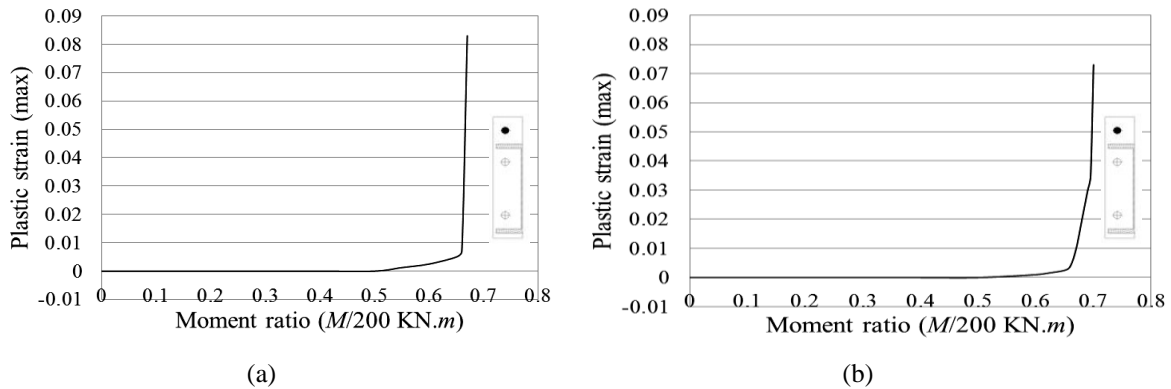


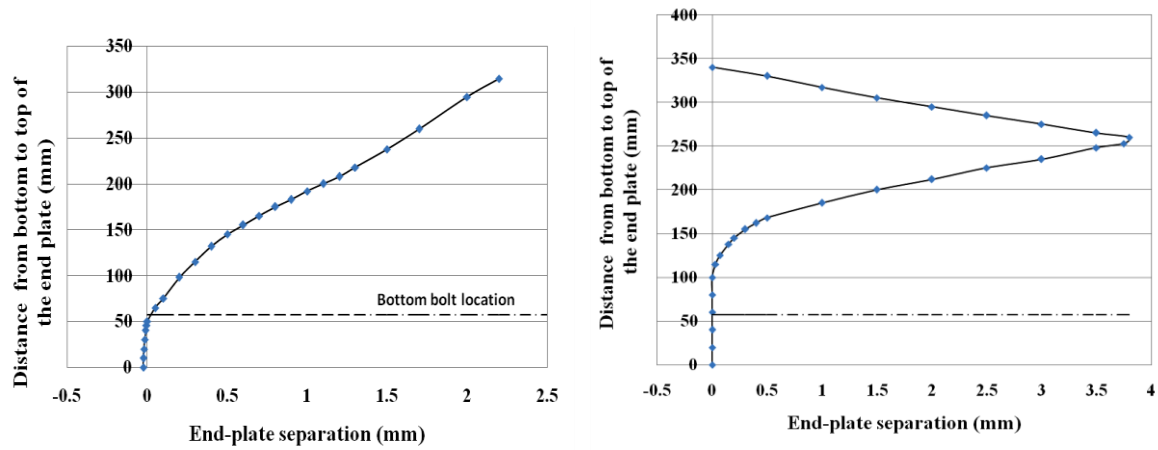
Fig. 7 Plastic strain vs. applied moment in (a) ct1a1, (b) ct1b6, for upper bolt

be studied in detail. The force in bottom bolts remained almost constant during the loading, which is about the initial pretensioning force. As it is expected, the bottom bolt forces increased instantly at the end of analysis, which was due to the connection failure. The forces in the upper bolts are different and they are more critical being closer to the tensile flange force of the bending moment and they are the ones controlling the ultimate state of the connection. The effective stress in three different nodes of the upper bolts is shown in Fig. 6.

As illustrated, bolt forces initially have remained constant due to presence of pretension. Then by increasing bending moment, the force in tensile bolts has received to its maximum capacity of 713 MPa. Checking of bolt plastic strain demonstrates its sudden increase at the end of analysis; as shown in Fig. 7. This illustrates the fracture of all tensile bolts at the end of loading procedure.

The connection failure mode can be determined by looking into the endplate separation from column flange. The endplate separation of two connections (ct1a1 and ct1b6) in the final loading step is illustrated in Fig. 8.

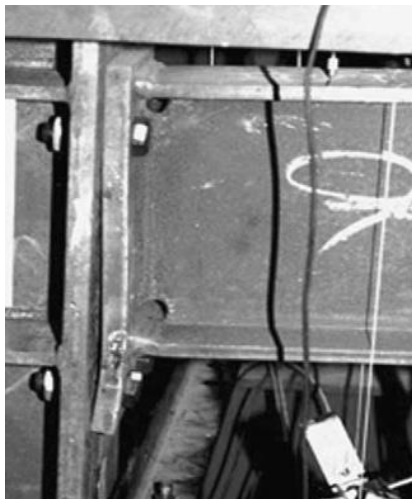
In ct1a1 connection, the endplate separation is shown from bottom bolts to the top edge of endplate. As expected, no prying force in the bolts is observed in ct1a1 connection and therefore the connection is considered as a thick endplate moment connection. It is observed from Fig. 8-b that



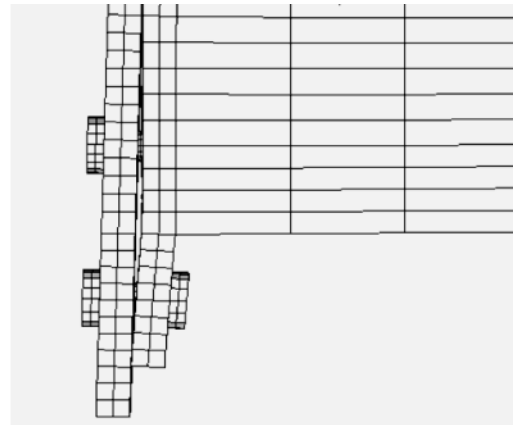
(a)

(b)

Fig. 8 Endplate separation (a) ct1a1, (b) ct1b6



(a)



(b)

Fig. 9 Endplate separation in ct1b6 (a) experiment (Maggi *et al.* 2004), (b) FEM

the endplate in ct1b6 connection has the highest separation where the tensile beam flange is located. While moment of the connection reaches its ultimate capacity, the tensile forces in the bolts reach their maximum forces and they will break. It can be easily inferred that the above connection is an endplate moment connection with intermediate thickness plate. Thus, there is a reasonable agreement between finite element and existing experimental results, which shows the accuracy of finite element analysis. In Fig. 9 the typical separations from experiment (Maggi *et al.* 2004) and from finite element method of analysis in ct1b6 connection are presented.

Fig. 10 shows the typical moment versus rotation of the connections. In this diagram, the connection rotation is obtained from dividing the endplate separation at the tensile beam flange by

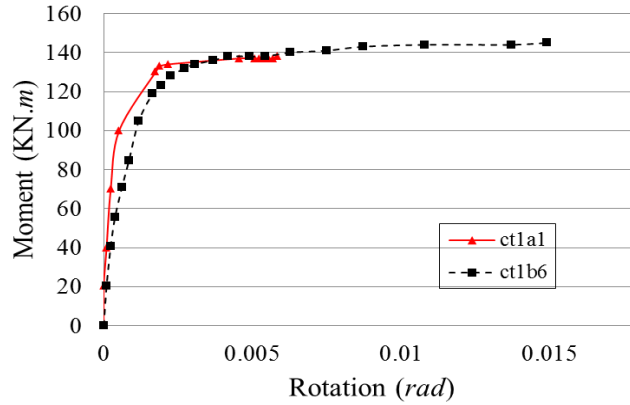


Fig. 10 Predicted moment vs. rotation in ct1a1 and ct1b6 connections

Table 2 Predicted ultimate moment and rotation capacity of connections

	Initial Stiffness (KN.m/rad)	FEM M_u (KN.m)	FEM Ultimate Rotation (rad)	Moment Ratio (FEM/Experiment)	Rotation Ratio (FEM/Experiment)	capacity of the connecting beam (KN.m)
ct1a1	3.89×10^5	136.8	0.0059	0.95	0.39	$171 > 136.8$
ct1b6	1.6×10^5	144	0.0149	1.052	2.534	$171 > 144$

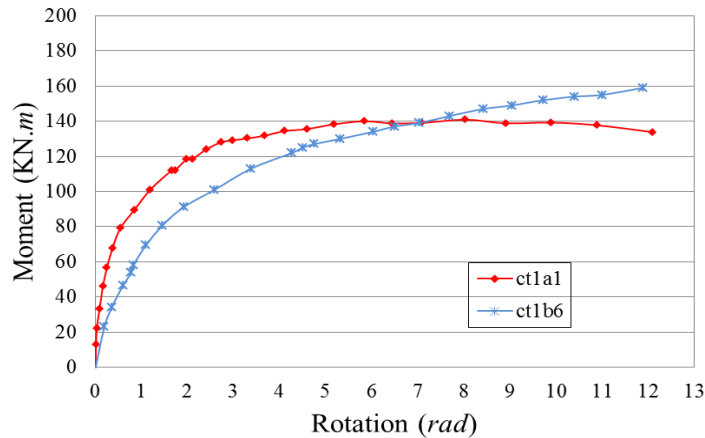


Fig. 11 Moment vs. rotation in ct1a1 and ct1b6 from experiment (Maggi *et al.* 2004)

the distance between centers of beam flanges. Comparison of two ct1a1 and ct1b6 connections shows that ct1b6 connection has evidently more rotational capacity. However, the ultimate moment capacities of these two connections are almost the same. This comparison between ultimate moment and rotation capacity of connections is shown in Table 2.

Good correlation between predicted finite element and experimental results is observed (Figs. 10 and 11). However, comparing the predicted results with the experimental results further, although there is a slight difference in the initial bending stiffness of the connections, the overall predicted bending resistance matches very well with the experimental ones.

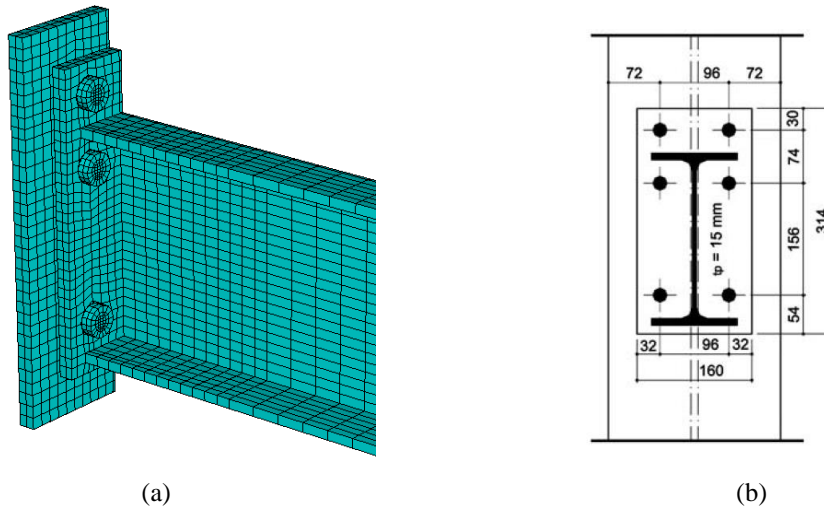


Fig. 12 (a) Typical FEM mesh and (b) End plate Configuration (De Lima *et al.* 2004)

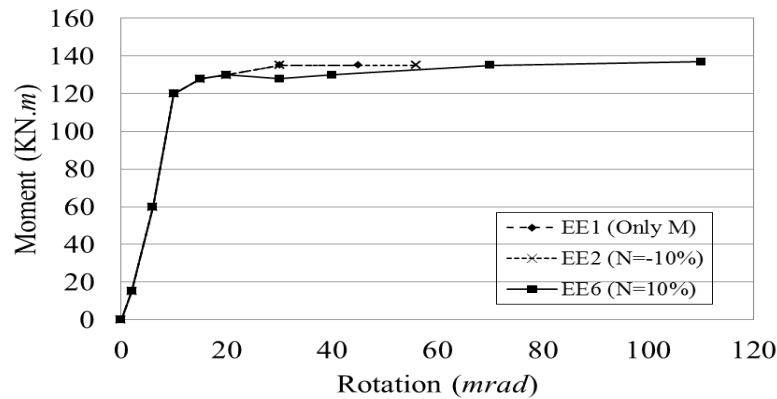


Fig. 13 Moment vs. rotation results from finite element analysis.

4. Finite element model calibration for axial force implementation

One connection subjected to axial force and bending moment is considered as a benchmark case for investigating the accuracy of finite element analysis results. For this purpose, the connection tested by De Lima *et al.* (2004) is modeled and analyzed, and the results obtained are compared with existing experimental results. The model comprises IPE240 beam connected to HEB240 column (Fig. 12).

In this connection, endplate has 15 mm thickness, 160 mm width and 314 mm height with three rows of two bolts. Endplate, beam, and column are all S275 steel; having 360 MPa yield strength and 460 MPa ultimate strength. Bolts are M20, which are steel grade 10.9. The pretensioning stress in bolts, which is being applied by thermal gradient, is 630 MPa. The connection is analyzed with different axial forces such as no axial force or with axial force equivalent to tensile force of $0.1F_{y-beam}$ or compressive force of $-0.1F_{y-beam}$; in which $1F_{y-beam}$ is the beam yield strength capacity.

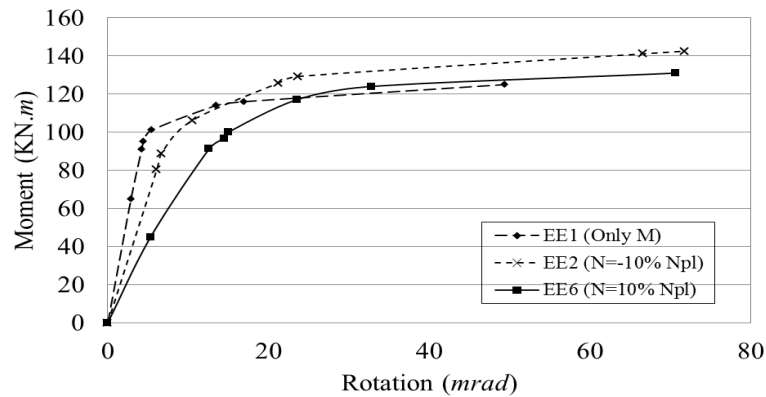


Fig. 14 Moment vs. rotation results from experiment (De Lima *et al.* 2004)

Moment versus rotation diagrams are presented in Fig. 13 from finite element analysis.

The rotation of connection is obtained from dividing the vertical displacement of the beam tip by the beam length plus the column flange thickness. Comparing the results obtained for FEM, as presented in Fig. 13, by the results obtained for experiment, as presented in Fig. 14, a good agreement between experimental and analytical results is observed, which shows the accuracy of finite element analysis conducted on this model and previous models (Fig. 14).

5. Behavior of connection subjected to axial force and bending moment

After exploration of moment behavior of two aforementioned connections and verification of FEM analysis results, the behavior of the connection subjected to simultaneous bending and axial force is investigated. The axial force is exerted to beam in the form of percentage of beam section tensile yield strength. Besides studying the influence of axial force on moment capacity of the connection, initial stiffness of the connection as well as diagnosing the failure modes are part of the investigations. After applying the axial forces, the bending moment is applied in small increments. The moment versus axial force interaction diagram is prepared by changing the axial force from the ultimate tensile limit to ultimate compressive limit in which at both cases the bending moment is zero. In Fig. 15, the variation of axial force with respect to moment capacity of the connection is shown. In this interaction diagram, the “Moment ratio” is obtained from dividing the ultimate moment of the connection with axial force by the ultimate moment of the connection without axial force. The stress ratio is provided from dividing exerted axial force (P) by beam section yield force. On the diagram presented the positive and negative signs present tensile and compressive nature of the axial forces.

Several behavioral domains are considerable in Fig. 15. On condition that there is no bending moment ($M=0$), the ultimate tensile capacity of the connection equals remaining tensile capacity of the bolts attending to pretension force value. In this case, the connection failure is controlled by remaining tensile capacity of the bolts. The moment capacity of connection increases by reducing the tensile axial force, since the tensile bolts control connection failure. Therefore reduction of tensile axial force increases the moment capacity of the connection. In other words, by increasing tensile axial force, the moment capacity decreases.

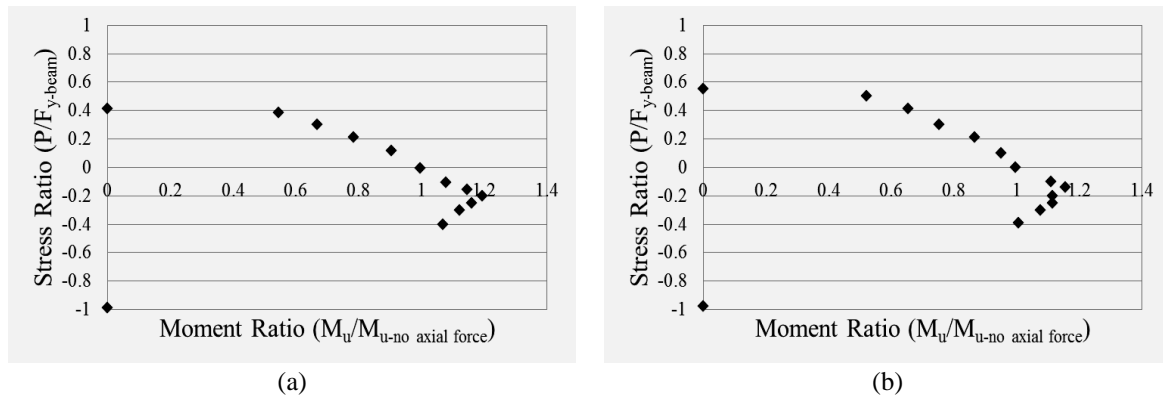


Fig. 15 Moment vs. axial force in; (a) ct1a1, (b) ct1b6

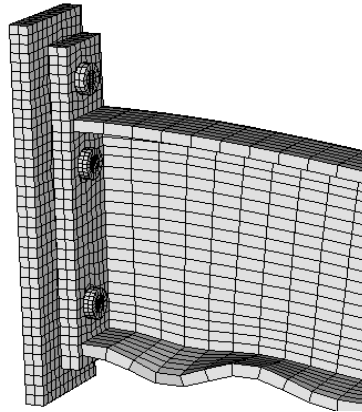


Fig. 16 Typical compressive beam flange buckling in ct1b6 connection

In case, the compressive axial force is applied, connection moment capacity is initially increased by increasing the axial force. In this situation, the tensile bolt capacity controls the connection failure. Therefore, increase in compressive axial force provides an additional capacity for connecting bolts (tensile bolts) and thereupon for the connection. By continuing the increase of compressive axial force at the point that the force is near $(0.15-0.2)F_{y-beam}$ in both connections, the moment capacity reaches its maximum value, and then it is reduced by increasing compressive axial force. This decrease in moment capacity is due to the occurrence of compressive beam flange buckling (Fig. 16).

After this point, by increasing the compressive axial force, moment capacity decreases since in these situations the connection failure is in type of compressive beam flange buckling. Finally, ultimate compressive capacity of the connection (without bending moment), which is the beam section yield strength, is acquired. In the models that tensile axial force is equivalent to $0.2F_{y-beam}$, the moment capacity is reduced by 17%. In fact, by using the tensile axial force in a small value, the reduction in moment capacity is noticeable. Moreover, in compressive axial force of $(0.15-0.2)F_{y-beam}$, the connection moment capacity has increased by 1.16 to 1.19 times of moment capacity of the connection without axial force. Comparing the interaction diagram obtained from

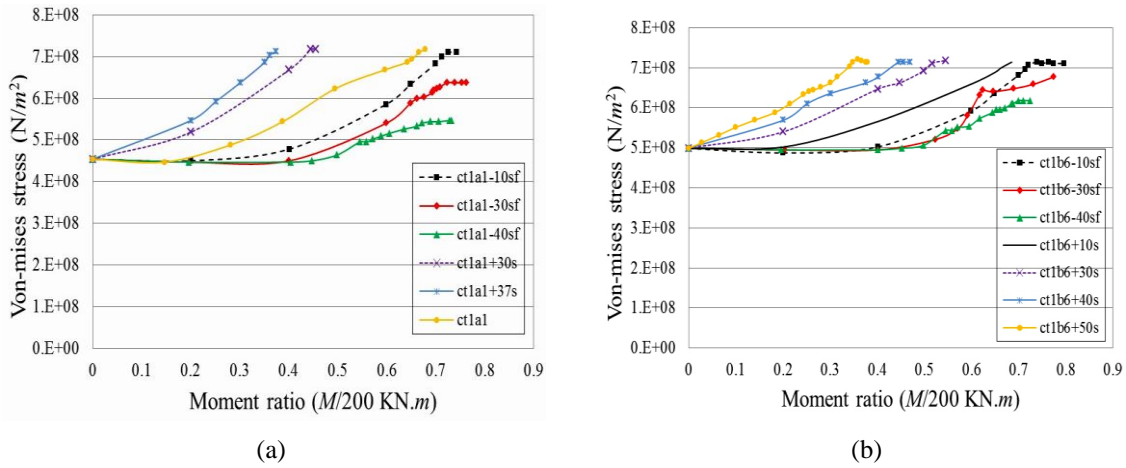


Fig. 17 Von-Mises stress vs. applied moment and axial force (a) ct1a1, (b) ct1b6

this research with the one suggested in Eurocode3, then it is noted that the predicted interaction diagram is nonlinear while the Eurocode3 interaction diagram is linear in every part and in most cases produce conservative results. For instance, as shown in Fig. 15, for the two specific experimental cases considered, our results show that up to 20% of the compressive axial force, the bending resistance increases by almost 1.2 times in comparison with the case in Eurocode3. Thus, up to 20 percent increase in the capacity of the connection is being demonstrated with respect to the Eurocode3.

It was understood that the presence of axial force has a noticeable effect on ultimate moment resistant of the connection. Additionally it causes appearance of different failure mode; which indicates that the effect of axial force on the bolts must be investigated. The variation of the upper bolt stresses are shown in Fig. 17.

In the figure presented, “sf” index in the model title indicates that lateral stiffener has been used on the beam tip near where the load is applied to prevent the lateral buckling of the beam during loading. In addition, it explains that finer mesh has been used at the end of the beam where the bulking may occur. “s” index in the model title indicates that lateral stiffener is used with coarser mesh. The numeral coefficient in model title expresses the percentage of applied axial force with respect to the beam tensile yield strength.

In ct1a1 connection, stress in upper bolts reaches its maximum value (713 Mpa) in all cases in which the axial force are tensile forces, or compressive axial force of $-0.1F_{y-beam}$, $-0.15F_{y-beam}$, and $-0.2F_{y-beam}$ at ultimate moment capacity. Consequently, in these connections, the failure is due to tensile bolt yielding. By increasing the compressive axial force, at ultimate moment level, the stress in upper bolts successively reduces because the beam flange bulking occurs prior to bolt yielding in those cases. As a result, by increasing axial force which leads to reduction of moment capacity, the stress in tensile bolts reduces more than before. In ct1b6 connection, stress in upper bolts reach their maximum level in all cases with tensile axial force and compressive axial forces of $-0.1F_{y-beam}$, $-0.15F_{y-beam}$, $-0.2F_{y-beam}$, and $-0.25F_{y-beam}$. The stress in the upper bolts decrease by increasing the compressive axial force because of beam flange buckling. At tensile axial forces equal to $0.4F_{y-beam}$ and $0.5F_{y-beam}$, the axial force neutralizes the effect of pretension; and therefore the stress in upper bolts increase once bending moment is applied.

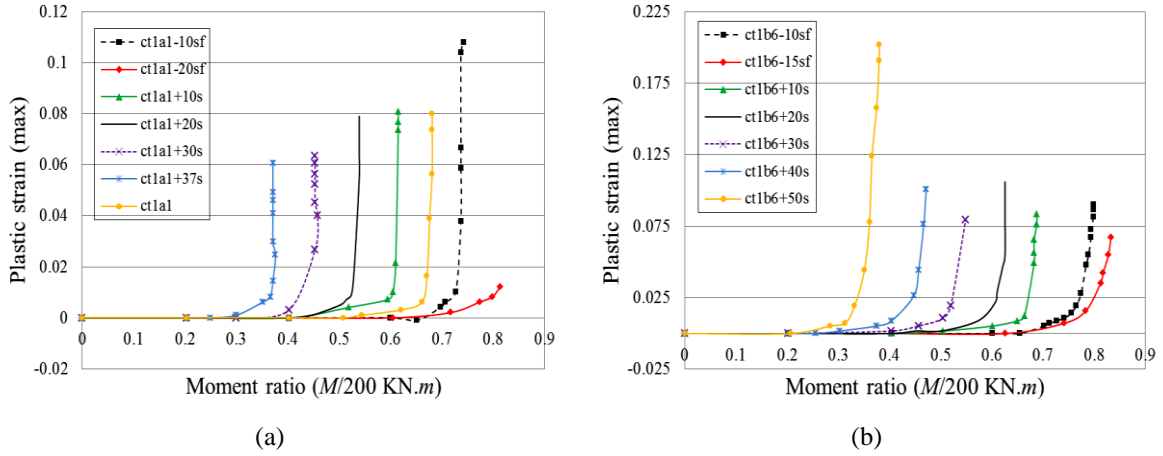


Fig. 18 Plastic strain vs. moment in upper bolt in (a) ct1a1, (b) ct1b6, with axial force

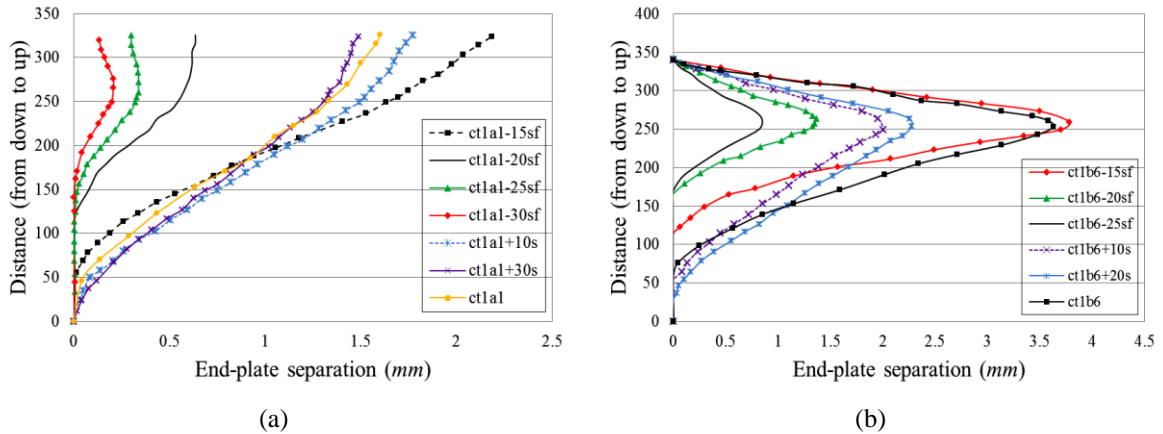


Fig. 19 Endplate separation vs. moment in (a) ct1a1, (b) ct1b6, with axial force

Studying the bolt strain can be useful for measuring the influence of axial forces on plasticity of bolts (Fig. 18).

In ct1a1 connection, the plastic strain in bolts is almost zero on compressive axial force equivalent to $-0.3F_{y-beam}$ and $-0.4F_{y-beam}$; which indicates they remained elastic, and are omitted from the diagram. In ct1b6 connection, the upper bolts experienced plasticity in all cases except in $-0.4F_{y-beam}$ compressive axial force in which they remained elastic. Finally, the maximum plastic strain is achieved at $0.5F_{y-beam}$ of tensile axial force.

We can identify the location of neutral axis as well as endplate deformation by studying the pattern of endplate separation at different stage; which can also be used for understanding the force distribution in bolts. In Fig. 19 the endplate separation is shown for different type of axial forces. In ct1a1 connection, under compressive axial force in all cases, which the failure mode is of beam flange buckling, the endplate separation has decreased intensely. The separation in other models is approximately identical, and only the neutral axis is dislocated. In both connections, the maximum separation is observed at $-0.15F_{y-beam}$ of compressive axial force. In ct1b6 connection, the minimum

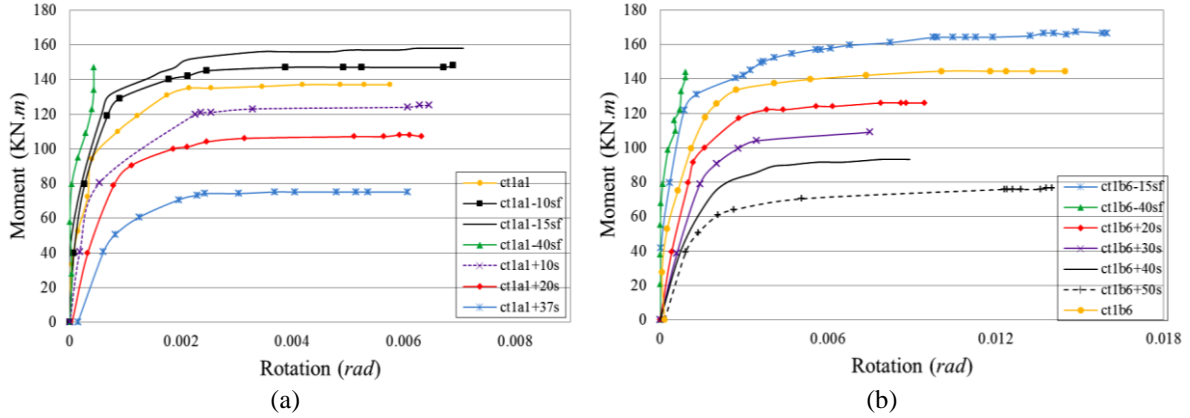


Fig. 20 Endplate rotation vs. moment in (a) ct1a1, (b) ct1b6, with axial force

Table 3 Initial moment stiffness of the ct1a1 connection with axial force

Model	ct1a1	ct1a1-10sf	ct1a1-15sf	ct1a1-20sf	ct1a1-25sf	ct1a1-30sf
Initial stiffness (KN.m/rad)	3.89×10^5	6.8×10^5	1.0×10^6	2.0×10^6	2.0×10^6	3.0×10^6
Moment Capacity (KN.m)	136.8	148	158	163	160	153
Rotation Capacity (rad.)	0.0059	0.0068	0.0071	0.0025	0.0014	0.0009
Model	ct1a1-40sf	ct1a1+10s	ct1a1+20s	ct1a1+30s	ct1a1+37s	–
Initial stiffness (KN.m/rad)	4.0×10^6	2.41×10^5	1.65×10^5	1.2×10^5	0.95×10^5	–
Moment Capacity (KN.m)	146	125	107	91	75.1	–
Rotation Capacity (rad.)	0.0004	0.0070	0.0065	0.0057	0.0060	–

Table 4 Initial moment stiffness of the ct1b6 connection with axial force

Model	ct1b6	ct1b6-10sf	ct1b6-15sf	ct1b6-20sf	ct1b6-25sf	ct1b6-30sf
Initial stiffness (KN.m/rad)	1.6×10^5	2.1×10^5	5.07×10^5	7.45×10^5	1.0×10^6	2.0×10^6
Moment Capacity (KN.m)	144	159	167	161	160	156
Rotation Capacity (rad.)	0.0149	0.0152	0.0161	0.0057	0.0038	0.0024
Model	ct1b6-40sf	ct1b6+10s	ct1b6+20s	ct1b6+30s	ct1b6+40s	ct1b6+50s
Initial stiffness (KN.m/rad)	4.0×10^6	1.08×10^5	0.83×10^5	0.87×10^5	0.63×10^5	0.46×10^5
Moment Capacity (KN.m)	145	137	125	109	94	76
Rotation Capacity (rad.)	0.0008	0.0090	0.0097	0.0078	0.0092	0.014

separation, which was due to the flange buckling, is observed at compressive axial force of $-0.2F_{y-beam}$ and higher.

In Fig. 20(a), the moment versus rotation diagram of ct1a1 connection is presented. It can be understood that the lowest initial stiffness correlates to tensile axial force equivalent to $0.37F_{y-beam}$ since in this case there is no pretension at the beginning of moment loading procedure (Fig. 17(a)). By applying the compressive axial force in connections, the initial stiffness has been increased in comparison with the initial stiffness of connections without axial force. In addition, the maximum rotation is observed at $-0.1F_{y-beam}$ and $-0.15F_{y-beam}$ of compressive axial force. Then by increasing the compressive axial force, an intense decrease in connection rotation occurs, which is due to the

change in failure mode of the connection. In the models with tensile axial force, the ultimate rotation nearly remains constant, which is about ultimate rotation of the connection without axial force, and the initial stiffness remains lower than initial stiffness of the connection without axial force. In ct1b6 connection under tensile axial force (Fig. 20(b)), the initial stiffness is less than initial stiffness of the connection without axial force, which presents that the presence of tensile axial force on bolts lowers the influence of pretension. On the contrary, the initial stiffness increases by applying the compressive axial force and the maximum rotation occurs on axial force equal to $-0.15F_{y-beam}$.

Under tensile axial force, the ultimate rotation capacity of connections, except at the model with $0.5F_{y-beam}$ axial force, remains considerably less than its amount in connection without axial force. The numerical values of initial stiffness as well as the connection capacity are presented in Table 3 and 4. As shown previously in Fig. 15, the moment capacity of connection increases by reducing the tensile axial force, and for compressive axial force, connection moment capacity is initially increased and then decreased by increasing the axial force. This trend can be observed in Fig. 20 and Tables 3 and 4.

6. Conclusions

The nonlinear static analysis of the end plate moment connections with different configuration showed that the finite element results have a suitable correlation with the results obtained from previous experiments. From the results obtained, it was understood that the numerical procedure which predicts the connection failure mode, are correct. Application of axial force on connections with thick or intermediate thickness endplates, showed that in all of the tensile axial force loading cases, the ultimate moment capacity decreases by increasing axial force. The moment capacity reduction is expected due to bolts failure in tension. In contrary to the tensile cases, by increasing compressive axial force, initially the moment capacity increased but in continuance, the moment capacity decreased due to occurrence of different failure mode in type of beam flange bulking. After this point, flange buckling was observed in all of the axial and bending moment load combinations. Because of the noticeable effect of axial force on beams, it must be considered on assessment of ultimate moment capacity of connection. In connection with thick endplate, in all of the axial force loading cases except those that cause beam flange buckling in combination with bending moment, the ultimate rotation was nearly equal to ultimate rotation of connection with no axial force. In connection with intermediate endplate thickness under tensile axial force, except axial force of half of beam yield strength, and compressive axial force, that causes beam flange buckling in combination with bending moment, the connection rotation declines in comparison with rotation of connection with no axial force. In all the connections considered, the maximum moment was observed on compressive axial force equivalent to 15% of beam section yield stress.

References

- ABAQUS User's Manual (2003), Version 6.4, ABAQUS Inc., Providence, R.I.
- Adey, B.T., Grondin, G.Y. and Cheng, J.J.R. (1998), "Extended endplate moment connections under cyclic loading", *J. Constr. Steel Res.*, **46**(1-3), 435-446.
- Adey, B.T., Grondin, G.Y. and Cheng, J.J.R. (2000), "Cyclic loading of endplate moment connections", *Can. J. Civil Eng.*, **27**(4), 683-701.

- Aggarwal, A.K. (1994), "Comparative tests on endplate beam-to-column connections", *J. Constr. Steel Res.*, **30**, 151-175.
- Ahuja, V., Kukreti, A.R. and Murray, T.M. (1982), "Analysis of stiffened endplate connections using the finite element method", Research Report No. FSEL/MBMA 82-01, Fears Structural Engineering Laboratory, School of Civil Engineering and Environmental Science, University of Oklahoma, Norman, Oklahoma.
- ANSI/AISC 358-05 (2005), "Prequalified connections for special and intermediate steel moment frames for seismic applications", American Institute of Steel Construction, Chicago, Illinois, USA.
- Bahaari, M.R. and Sherbourne, A.N. (1994), "Computer modeling of an extended endplate bolted connection", *Comput. Struct.*, **52**(5), 879-893.
- Bond, D.E. and Murray, T.M. (1989), "Analytical and experimental investigation of a flush moment endplate connection with six bolts at the tension flange", Research Report No. CE/VPI-ST-89/10, Dept. of Civil Engineering, Virginia Polytechnic Institute and State University, Blacksburg, VA.
- Borgsmiller, J.T. (1995), "Simplified method for design of moment endplate connections", M.S. Thesis, Department of civil Engineering, Virginia Polytechnic Institute and State University, Blacksburg, Virginia.
- Bose, B., Wang, Z.M. and Sarkar, S. (1997), "Finite-element analysis of unstiffened flush endplate bolted joints", *J. Struct. Eng.*, **123**(12), 1614-1621.
- Coelho, A.M.G., Bijlaard, F.S.K. and Da Silva, L.S. (2004), "Experimental assessment of the ductility of extended endplate connections", *Eng. Struct.*, **26**(9), 1185-1206.
- Coelho, A.M.G. and Bijlaard, F.S.K. (2007), "Experimental behavior of high strength steel endplate connections", *J. Constr. Steel Res.*, **63**, 1228-1240.
- Da Silva, L. (2008), "Towards a consistent design approach for steel joints under generalized loading", *J. Constr. Steel Res.*, **64**(9), 1059-1075.
- Da Silva, L., De Lima, L.R.O., Vellasco, P.C.G. and De Andrade, S.A.L. (2004), "Behaviour of flush endplate beam-to-column joints under bending and axial force", *Int. J. Steel Compos. Struct.*, **4**(2), 77-94.
- De Lima, L.R.O., Da Silva, L., Vellasco, P.C.G. and De Andrade, S.A.L. (2004), "Experimental evaluation of extended endplate beam-to-column joints subjected to bending and axial force", *Eng. Struct.*, **26**(10), 1333-1347.
- Diaz, C., Victoria, M., Marti, P. and Querin, O.M. (2011), "FE model of beam-to-column extended endplate joints", *J. Constr. Steel Res.*, **67**(10), 635-649.
- Eurocode 3 (1993), Design of steel structures: Part 1.1-General rules and rules for buildings - Revised annex J: Joints in building frames, European Pre-norm, CEN, Brussels, Europe.
- Ghassemieh, M., Kukreti, A.R. and Murray, T.M. (1983), "Inelastic finite element analysis of stiffened endplate moment connections", Research Report No. FSEL/MBMA 83-02, Fears Structural Engineering Laboratory, School of Civil Engineering and Environmental Science, University of Oklahoma, Norman, Oklahoma.
- Jaspart J.P., Braham M. and Cerfontaine, F. (1999), "Strength of joints subject to combined action of bending moments and axial forces", *Proceedings of the Conference Eurosteel '99*, **2**, CTU Prague, Prague.
- Krishnamurthy, N. and Graddy, D.E. (1976), "Correlation between 2- and 3-dimensional finite element analysis of steel bolted endplate connections", *Comput. Struct.*, **6**(4-5), 381-389.
- Lemonis, M.E. and Gantes, C.J. (2009), "Mechanical modeling of the nonlinear response of beam-to-column joints", *J. Constr. Steel Res.*, **65**(4), 879-890.
- Maggi, Y.I., Goncalves, R.M., Leon, R.T. and Ribeiro, L.F.L. (2004), "Parametric analysis of steel bolted endplate connections using finite element modeling", *J. Constr. Steel Res.*, **61**(5), 689-70.
- Mann, A.P. (1968), "Plastically designed endplate connections", Ph.D. Thesis, University of Leeds, England.
- Mays, T.W. (2000), "Application of the finite element method to the seismic design and analysis of large moment end-plate connections", Ph.D. Dissertation, Virginia Polytechnic Institute and State University, Blacksburg, Virginia.
- Meng, R.L. (1996), "Design of moment end-plate connections for seismic loading", Ph.D. Dissertation Submitted to Virginia Polytechnic Institute and State University, Virginia Polytechnic Institute and State University, Blacksburg, Virginia.

- Murray, T.M. (1990), *AISC Design Guide Series 4, Extended Endplate Moment Connections*, American Institute of Steel Construction, Chicago.
- Murray, T.M. and Shoemaker, W.L. (2002), "Steel design guide series 16, flush and extended multiple-row moment endplate connections", American Institute of Steel Construction, Chicago, IL.
- Nogueiro, P., Da Silva, L., Bento, R. and Simoes, R. (2009), "Calibration of model parameters for the cyclic response of end-plate beam-to-column steel-concrete composite joints", *Steel Compos. Struct.*, **9**(1), 39-58.
- Sherbourne, A. (1961), "Bolted beam-to-column connections", *Struct. Eng.*, **39**(6), 203-210.
- Sokol, Z., Wald, F., Delabre, V., Muzeau, J.P. and Svarc, M. (2002), "Design of end plate joints subject to moment and normal force", *Proceedings of the Conference Eurosteel*.
- Sumner, E.A. and Murray, T.M. (2001), "Experimental investigation of four bolts wide extended endplate moment connections", Research Report No. CE/VPI-ST-01/15, Submitted to Star Building System, Inc., Oklahoma City, Oklahoma, USA.
- Urbonas, K. and Daniunas, A. (2006), "Behavior of semi-rigid steel beam-to-beam joints under bending and axial forces", *J. Constr. Steel Res.*, **62**(12), 1244-1249.
- Yang, C.M. and Kim, Y.M. (2007), "Cyclic behavior of bolted and welded beam-to-column joints", *Int. J. Mech. Sci.*, **49**(5), 635-649.